Earthq Eng & Eng Vib (2020) 19: 839-853 **DOI**: https://doi.org/10.1007/s11803-020-0599-1

# Resilience-based retrofitting of existing urban RC-frame buildings using seismic isolation

Yang Cantian[1†], Xie Linlin[2,3‡], Li Aiqun[1,2,3§], Zeng Demin[3§], Jia Junbo[3§], Chen Xi[4*] and Chen Min[3#]

1. *School of Civil Engineering, Southeast University, Nanjing 211189, China*
2. *The Research and Development Joint Center of Energy Dissipation Technology of Southeast University and Forceset Corporation, Southeast University, Nanjing 211189, China*
3. *School of Civil and Transportation Engineering, Beijing University of Civil Engineering and Architecture, Beijing 100044, China*
4. *Beijing Institute of Architectural Design, Beijing 100045, China*

**Abstract:** The improvement of the seismic resilience of existing reinforced-concrete (RC) frame buildings, which is essential for the seismic resilience of a city, has become a critical issue. Although seismic isolation is an effective method for improving the resilient performance of such buildings, target-oriented quantitative improvements of the resilient performance of these buildings have been reported rarely. To address this gap, the seismic resilience of two existing RC frame buildings located in a high seismic intensity region of China were assessed based on the Chinese Standard for Seismic Resilience Assessment of Buildings. The critical engineering demand parameters (EDPs) affecting the seismic resilience of such buildings were identified. Subsequently, the seismic resilience of buildings retrofitted with different isolation schemes (i.e., yield ratios) were evaluated and compared, with emphasis on the relationships among yield ratios, EDPs, and levels of seismic resilience. Accordingly, to achieve the highest level of seismic resilience with respect to the Chinese standard, a yield ratio of 3% was recommended and successfully applied to the target-oriented design for the seismic-resilience improvement of an existing RC frame building. The research outcome can provide an important reference for the resilience-based retrofitting of existing RC frame buildings using seismic isolation in urban cities.

**Keywords:** existing urban RC frame building; retrofitting using seismic isolation; seismic resilience; yield ratio

## 1 Introduction

Over the last 30 years, modern cities in China have seen an increase in the number of reinforced-concrete (RC) frame buildings, including hospitals, schools, offices, and government buildings, which are essential for the seismic resilience of a city. To evaluate and improve the seismic resilience of a city, it is necessary to first quantify the seismic resilience of typical existing RC frame buildings and identify the critical factors affecting it. Furthermore, a reliable and high-efficiency method must be recommended to control such critical factors and improve the seismic resilience of such buildings.

Various seismic-resilience-assessment methods have been proposed to evaluate the performance or guide the design of buildings (Bruneau *et al*., 2003; Cimellaro *et al*., 2010, 2017; FEMA, 2012; Hu *et al*., 2017; Renschler *et al*., 2010; Almufti and Willford, 2013; Zhou *et al*., 2017, 2019, 2020). A city-scale seismic-resilience-assessment method was creatively proposed by Xiong *et al*. (2020). However, these methods cannot be used directly for assessing the seismic resilience of buildings in China. This is because the component fragility data and loss functions of various countries exhibit significant differences. To address this issue, the Standard for Seismic Resilience Assessment of Buildings GB/T 18591-2020 (MOHURD, 2020), which is referred to as "the standard" hereafter, was issued in 2020 and is the first Chinese national standard focused on seismic resilience of buildings. This standard includes the fragility database and loss functions of critical components of the buildings of China. Furthermore, a seismic-resilience-assessment method and the corresponding program were also developed based on the standard and then released.

**Correspondence to**: Xie Linlin, The Research and Development Joint Center of Energy Dissipation Technology of Southeast University and Forceset Corporation, Southeast University, Nanjing 210096, China
Tel: +86-15652316896
E-mail: xielinlin@bucea.edu.cn
[†]PhD Candidate; [‡]Associate Professor; [§]Professor; [*]Senior Engineer; [#]Former graduate student

**Supported by:** Beijing Natural Science Foundation under Grant No. 8192008, the Scientific Research Foundation of Graduate School of Southeast University under Grant No. YBPY2021, the Science and Technology Project of Beijing Municipal Education Commission under Grant No. KM201910016014, and the Program for Changjiang Scholars and Innovative Research Team in University under Grant No. IRT_17R06
**Received** May 1, 2020; **Accepted** July 7, 2020

However, investigations of the seismic resilience of existing buildings based on this standard are rarely reported. To yield more realistic results reflecting the typical situation of buildings in China and to provide a valuable reference on the application of the standard, the seismic-resilience assessment of existing RC frame buildings is valuable to be conducted. In addition, the critical factors that affect the levels of seismic resilience must be identified for achieving the subsequent improvements.

Seismic isolation technology is acknowledged as the most effective method for improving the seismic performance of buildings and is therefore widely adopted in the retrofitting of existing buildings (Moretti *et al*., 2014; Dong and Frangopol, 2016; Li, 2020; Matsagar and Jangid, 2008; Mayes *et al*., 2012; Yang *et al*., 2019; Zhou and Tan, 2018). Currently, various researchers have investigated the seismic resilience of isolated buildings and retrofitted buildings by using seismic isolation (Bhagat and Wijeyewickrema, 2017; Dong and Frangopol, 2016; Mayes *et al*., 2012; Shang *et al*., 2019; Taniguchi *et al*., 2016). Despite these efforts, previous studies were mostly based on an iterative design method. Specifically, a design scheme was first proposed, and then the corresponding seismic resilience was evaluated. If the expected target of resilience is not achieved, another scheme is introduced until the target is satisfied. This indicates that the scheme for retrofitting existing buildings cannot be directly designed toward a given target of seismic resilience. Note that different levels of seismic resilience with an emphasis on restoration cost, repair time and casualties are clarified in the standard. For the retrofitting of existing buildings using seismic isolation, a target-oriented quantitative improvement on the resilient performance of such buildings is preferred but is rarely reported.

To investigate a target-oriented method, it is necessary to know the relationship between the critical design parameters of the isolation system and the level of seismic resilience of the retrofitted building. The yield ratio of the isolation system (referred to as the "yield ratio" hereafter) is considered as a critical design parameter that significantly affects the efficiency of the isolation system and seismic performance of the entire building. It is defined as the ratio of the total yield force of the lead-rubber bearings ($Q_y$) to the total seismic weight of the structure ($W$) (Park and Otsuka, 1999; Pourzeynali and Zarif, 2008; Providakis, 2008; Avşar and Özdemir, 2013; Mollaioli *et al*., 2013; Li *et al*., 2017). Many researchers have correlated the seismic performance of a structure with its yield ratio and recommended rational values of the yield ratio, which targeted a given reduction ratio of the base shear force (Park and Otsuka, 1999; Pourzeynali and Zarif, 2008; Providakis, 2008; Mollaioli *et al*., 2013; Li *et al*., 2012; Li *et al*., 2017). Li *et al*. (2012) recommended the rational yield for isolated RC frame structures to be 3%–4.8%. Liu (2019) summarized the yield ratio of buildings in numerous reported engineering practices for isolated structures and indicated that yield ratios of 2%–5% were generally applied in engineering practices. Li *et al*. (2017) recommended the rational yield for isolated RC frame-core tube tall buildings to be 2%–3%. These recommendations shed light on this research, because it may be feasible to establish a relationship between the yield ratio and the seismic resilience of a retrofitted building.

To address the above-mentioned topics, the seismic resilience of two existing RC frame buildings located in a high seismic intensity region of China was assessed based on the Chinese Standard for Seismic Resilience Assessment of Buildings. The critical engineering demand parameters (EDPs) affecting the seismic resilience of such buildings were identified. Subsequently, the seismic resilience of such retrofitted buildings with different isolation schemes (i.e., yield ratios) were evaluated and compared, with emphasis on the relationships among yield ratios, EDPs, and seismic resilience level. Accordingly, to achieve the highest level of seismic resilience in the standard, a rational yield ratio was recommended and was successfully applied to the target-oriented design of the seismic resilience improvement of an existing RC frame building. The research outcome can provide an important reference for resilience-based retrofitting of existing RC frame buildings using seismic isolation in urban cities.

## 2 Seismic resilience assessment method of Chinese standard

As mentioned above, the Chinese standard, GB/T 18591-2020 (2020), is the first Chinese national standard focused on seismic resilience of buildings. The method regulated by the standard is adopted here to assess seismic resilience. According to the standard, the seismic resilience of buildings is evaluated based on critical indices relating to three aspects: restoration cost, repair time, and casualties. Each evaluation result of these critical indices is divided into four levels, and the resilience level of the building is determined as the lowest level of these three aspects. The evaluation procedure of the proposed method specified in the standard is schematically illustrated in Fig. 1 and explained in the subsequent seven steps.

(1) Collect building information, including the basic information (e.g., the height and area of each floor) as well as the quantities, types, and parameters of structural and non-structural components.

(2) Establish the finite element (FE) model of the building and perform nonlinear time-history analyses (NTHAs) under the design basis earthquake (DBE) and maximum considered earthquake (MCE). Eight natural and three artificial ground motions are required to be selected according to the design spectrum.

(3) Determine whether the building is worth repairing based on the residual inter-story drift ratio (RIDR). The

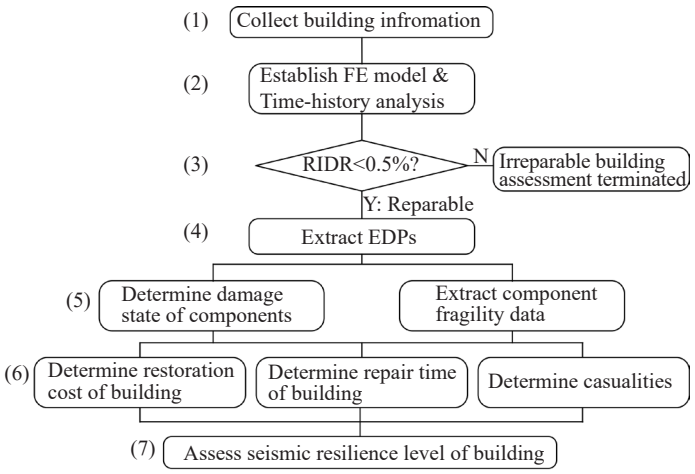


**Fig. 1 Evaluation method in standard for seismic resilience assessment of buildings**

upper threshold of RIDR is recommended to be 0.5% for RC and steel buildings.

(4) Extract EDPs obtained from NTHAs.

(5) Determine the damage states of components according to EDPs and fragility data.

(6) Determine the indices of the restoration cost ($\kappa$), repair time ($T_{tot}$), and casualties ($\gamma_H$ and $\gamma_D$) of the building according to the damage state of the components. The index of restoration cost, $\kappa$, is defined as the ratio of the restoration cost to the current replacement cost of the building. The repair time index, $T_{tot}$, is defined as the total time of the repair process, in which impeding factors are not considered. The indices of casualties, $\gamma_H$ and $\gamma_D$ are defined as the proportions of people who were hurt and died in the building, respectively.

(7) Evaluate the levels of the restoration cost, repair time, and casualties according to the principles listed in Tables 1–3. Then, the resilience level of the building is determined as the lowest level of these three aspects.

It is noteworthy that the standard requires the indices to be 84% of the percentile values obtained through the Monte Carlo analysis with samples of more than 1000.

## 3 Seismic resilience assessments of two existing RC frame buildings

Many RC frame buildings in the urban areas of China were built in the last 30 years. The seismic resilience of such buildings must be investigated and possibly improved. To reveal the seismic resilience of the existing RC frame buildings in modern cities, the seismic resilience of two buildings in real engineering projects located in Beijing were assessed using the above-mentioned method.

### 3.1 Building information on the studied RC frame buildings

The selected real engineering projects, namely Buildings A and B, are existing office buildings in Beijing, as detailed in Table 4. The three-dimensional and planar views of the buildings are presented in Fig. 2. The corresponding design seismic intensity is 8 degree according to the Chinese Code for Seismic Design of Buildings GB 50011-2010 (MOHURD, 2016), indicating that the corresponding peak ground accelerations (PGAs) of the DBE (i.e., 10% probability of exceedance in 50 years) and MCE (i.e., 2% probability of exceedance in 50 years) are 200 and 400 cm/s$^2$, respectively. The site condition belongs to Site Class II and is the second group in GB50011-2010. The characteristic period of the site is 0.40 s.

### 3.2 Building A

3.2.1 Component information

The component information for Building A was obtained from the design information archives and site investigation. Tables 5 and 6 respectively present the information on structural components (SCs) and non-structural components (NSCs) for Building A. According to the standard, the maximum inter-story drift

**Table 1 Principle for determining the level of restoration cost**

| Level | Earthquake level | Index of restoration cost, $\kappa$ |
|---|---|---|
| 3 | MCE | $\kappa \leq 5\%$ |
| 2 | MCE | $5\% < \kappa \leq 10\%$ |
| 1 | DBE | $\kappa \leq 10\%$ |
| 0 | DBE | $\kappa \geq 10\%$ |

**Table 2 Principle for determining the level of repair time**

| Level | Earthquake level | Index of repair time, $T_{tot}$ (day) |
|---|---|---|
| 3 | MCE | $T_{tot} \leq 7$ |
| 2 | MCE | $7 < T_{tot} \leq 30$ |
| 1 | DBE | $7 < T_{tot} \leq 30$ |
| 0 | DBE | $T_{tot} \geq 7$ |

**Table 3 Principle for determining the level of casualties**

| Level | Earthquake level | Indices of casualties, $\gamma_H$ and $\gamma_D$ |
|---|---|---|
| 3 | MCE | $\gamma_H \leq 10^{-4}$, and $\gamma_D \leq 10^{-5}$ |
| 2 | MCE | $\gamma_H \leq 10^{-3}$, and $\gamma_D \leq 10^{-4}$ |
| 1 | DBE | $\gamma_H \leq 10^{-3}$, and $\gamma_D \leq 10^{-4}$ |
| 0 | DBE | $\gamma_H \geq 10^{-3}$, or $\gamma_D \geq 10^{-4}$ |

**Table 4 Information of Building A and Building B**

| Index | Building A | Building B |
|---|---|---|
| Number of floors | 4 | 2 |
| Building height (m) | 14.7 | 8.82 |
| Height-to-width ratio | 0.45 | 0.36 |
| Building area (m$^2$) | 3952 | 1771 |
| Replacement cost (CNY) | 6,404,600 | 3,107,192 |

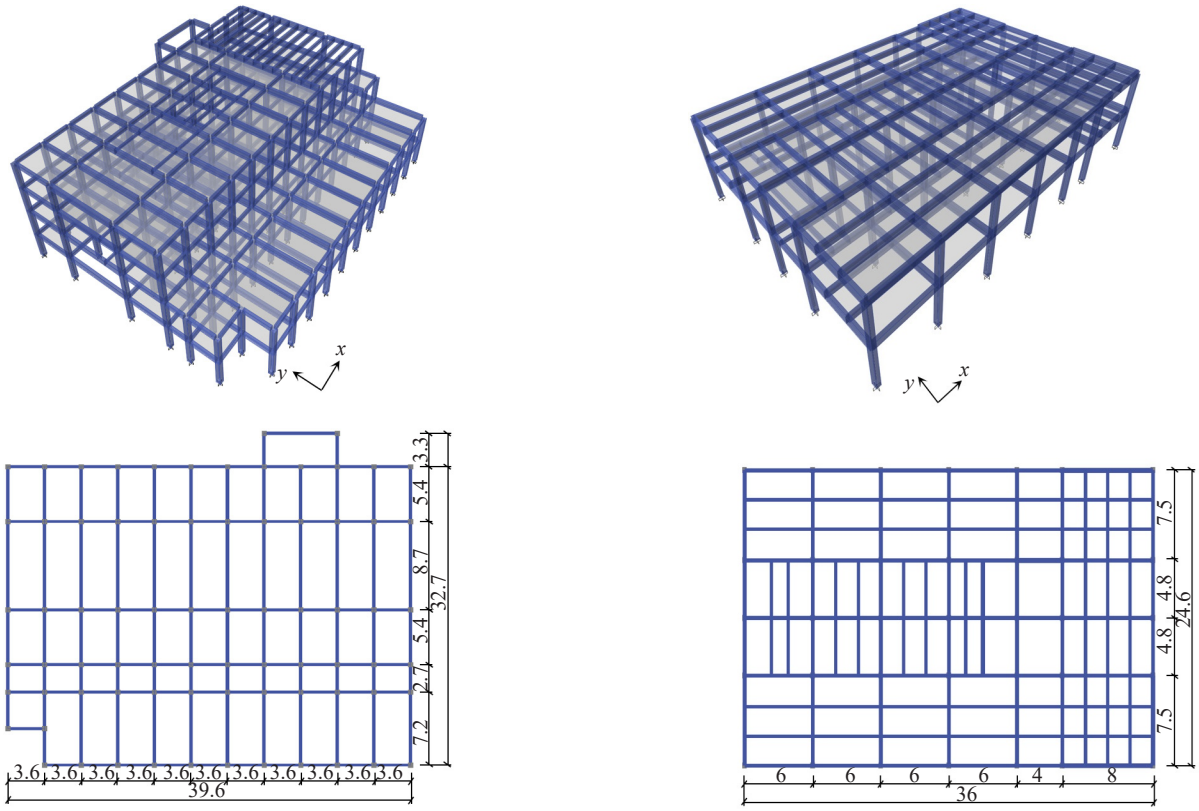


(a) Building A (b) Building B

**Fig. 2 Three-dimensional and planar views of Building A and Building B (unit: m)**

**Table 5 Structural component (SC) information of Building A**

| Type of component | Section dimension (mm × mm) | Fragility ID | Story | Quantity | | |
|---|---|---|---|---|---|---|
| | | | | *X* | *Y* | Non-directional |
| RC frame column | 500×500 | C.F.KZ | 1-2 | 0 | 0 | 75 |
| (Axial load ratio≤0.3) | 500×500 | C.F.KZ | 3 | 0 | 0 | 52 |
| | 500×500 | C.F.KZ | 4 | 0 | 0 | 46 |
| RC frame beam | 250×500 | C.F.KL | 1-2 | 66 | 0 | 0 |
| | 300×800 | C.F.KL | 1-4 | 1 | 0 | 0 |
| | 300×800 | C.F.KL | 1-2 | 0 | 26 | 0 |
| | 300×800 | C.F.KL | 1-2 | 0 | 22 | 0 |
| | 300×500 | C.F.KL | 1-2 | 0 | 19 | 0 |
| | 250×500 | C.F.KL | 3 | 45 | 0 | 0 |
| | 250×500 | C.F.KL | 3 | 11 | 0 | 0 |
| | 300×800 | C.F.KL | 3 | 0 | 26 | 0 |
| | 300×800 | C.F.KL | 3 | 0 | 9 | 0 |
| | 250×500 | C.F.KL | 3 | 0 | 6 | 0 |
| | 250×500 | C.F.KL | 4 | 38 | 0 | 0 |
| | 300×800 | C.F.KL | 4 | 13 | 0 | 0 |
| | 250×500 | C.F.KL | 4 | 10 | 0 | 0 |
| | 300×800 | C.F.KL | 4 | 0 | 22 | 0 |
| | 300×800 | C.F.KL | 4 | 0 | 8 | 0 |
| | 300×500 | C.F.KL | 4 | 0 | 4 | 0 |

ratio (MIDR) is the EDP that determines the damage state (DS) of columns and displacement-sensitive NSCs (DSNSCs). The EDP of the beam is the moment rotation of the beam hinge. In contrast, the DS of acceleration-sensitive NSCs (ASNSC) is determined using the EDP of maximum absolute floor acceleration (MAFA). Typical fragility curves of SCs and NSCs in Building A are presented in Fig. 3. Notably, different types of

**Table 6 Non-structural component (NSC) information of Building A**

| Type of component | Name | Fragility ID | EDP |
|---|---|---|---|
| Displacement-sensitive (DSNSC) | Stair | BI.S.02.01 | MIDR |
| | Glass curtain | BE.F.01.01 | MIDR |
| | Infill wall | BI.P.01.01 | MIDR |
| | Wall partition | BI.D.01.01 | MIDR |
| Acceleration-sensitive (ASNSC) | Ceiling | BI.C.01.01 | MAFA |
| | Chilled water piping | MEP.P.01.01 | MAFA |
| | Heating hot water piping 2 | MEP.P.02.01 | MAFA |
| | Heating hot water piping 1 | MEP.P.02.05 | MAFA |
| | Sanitary waste piping | MEP.P.03.01 | MAFA |
| | HVAC ducting | MEP.M.06.01 | MAFA |
| | Fire sprinkler piping | MEP.P.05.01 | MAFA |
| | Traction elevator | MEP.L.01.01 | MAFA |
| | Chiller | MEP.M.02.01 | MAFA |
| | Cooling tower | MEP.M.03.01 | MAFA |
| | Air handling unit | MEP.M.10.01 | MAFA |
| | Control cabinet | MEP.E.02.01 | MAFA |
| | Pendant lighting | BI.L.01.01 | MAFA |

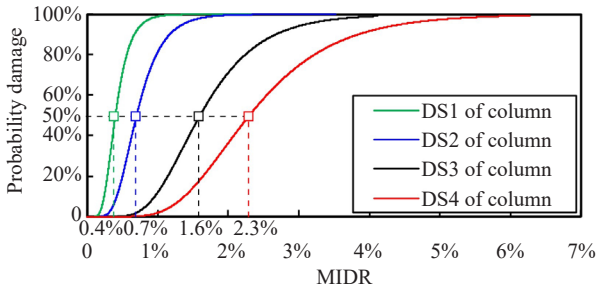


(a) Typical SC: RC frame column (C.F.KZ) with an axial load ratio lower than 0.3

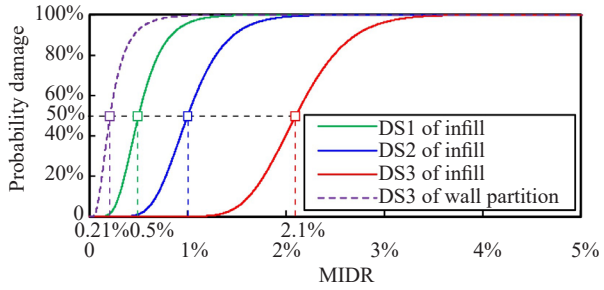


(b) Typical DSNSCs: Infill (BI.P.01.01) and wall partition (BI.D.01.01)

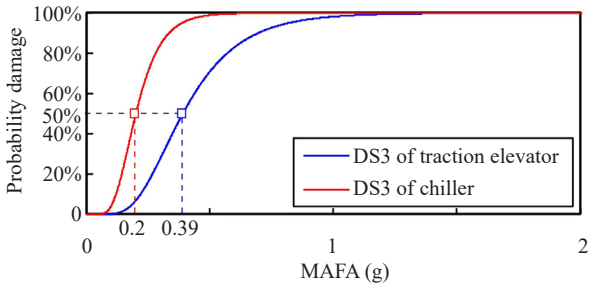


(c) Typical ASNSCs: Traction elevator (MEP.L.01.01) and chiller (MEP.M.02.01)

**Fig. 3 Fragility curves of typical components in Building A**

components may have different numbers of DSs. For example, the RC frame column has four DSs, whereas the wall partition and traction elevator have one DS each.

3.2.2 NTHA results of Building A

NTHA of Building A was conducted to obtain the EDPs. The commercial software, Perform-3D, was adopted to establish the nonlinear FE model. The well-acknowledged fiber model was used to simulate the RC frame components (Lu *et al*., 2015; Xie *et al*., 2015; Yang *et al*., 2019). The Penta- and tri-linear models were adopted for the concrete and reinforcement steel, respectively. The characteristic parameters of both the confined and unconfined concrete were calculated using the model proposed by Mander *et al*. (1988). A modal analysis was conducted before conducting the NTHAs. The first three periods are 0.597 s (1st-order translation in the *Y* direction), 0.508 s (1st-order translation in the *X* direction), and 0.471 s (1st-order torsion), respectively. The accuracy of the FE model was verified by comparing the modal analysis results of Perform-3D and ETABS (Computers and Structures Inc., 2003). The differences of the first three periods calculated with these two programs are below 3%. According to the requirements in the standard, eight natural ground motion records and three artificial ground motions were selected and generated to perform NTHAs and obtain the EDPs for resilience assessment. The response spectrum of each ground motion was then compared with the design response spectrum as shown in Fig. 4.

NTHAs under DBE and MCE were conducted using 11 ground motions as the seismic input to the structure along the direction of the fundamental modal (i.e., *Y*-axis). The maximum residual inter-story drift

ratio (MRIDR) was first checked to determine whether the building was worth repairing. For Building A, the MRIDRs were all less than 0.5%; thus, Building A was worth repairing and the assessment procedure could be conducted. Three types of EDPs, i.e., the MIDR, MAFA, and moment rotation of beam hinges, were obtained through NTHAs. The comparisons between the distributions of MIDR and MAFA under DBE and MCE are presented in Fig. 5. The MIDR appears at the second story with average values of 0.4% and 0.82% under DBE and MCE, respectively, whereas the MAFA was observed on the roof with average values of 0.40 and 0.61 g under DBE and MCE, respectively.

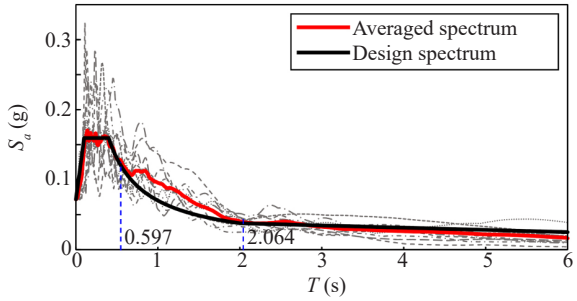


**Fig. 4 Comparison between the averaged spectrum and design response spectrum**

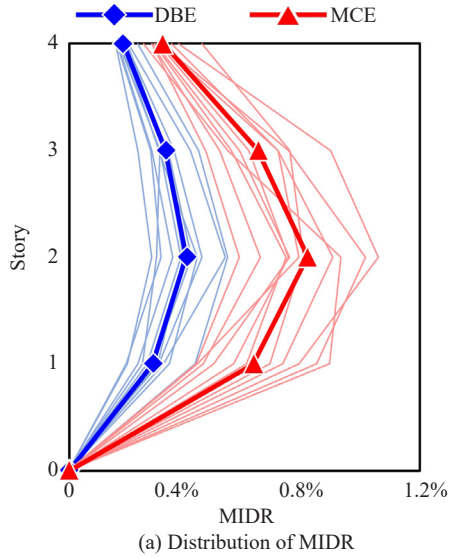


(a) Distribution of MIDR

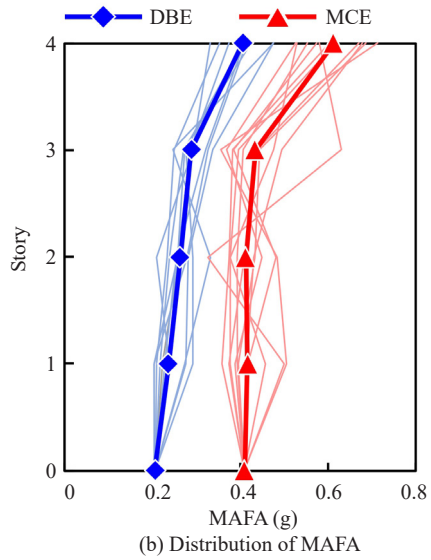


(b) Distribution of MAFA

**Fig. 5 Critical EDPs of Building A under DBE and MCE**

3.2.3 Seismic resilience assessment of Building A

3.2.3.1 Restoration cost

The restoration costs of SCs, DSNSCs, and ASNSCs under DBE and MCE are illustrated in Fig. 6. The composition of restoration costs is illustrated in Fig. 7. Notably, the values in Fig. 6 are the 84% percentile values of the Monte Carlo analyses, which is required by the standard to determine the level of restoration cost. In contrast, the values in Fig. 7 are calculated based on the averaged values collected from the Monte Carlo analyses conducted 1000 times; this could reflect the general trends (Tian *et al*., 2016). As such, the following findings can be drawn.

(1) The restoration costs under DBE and MCE were obtained as 292,500 and 918,300 CNY, respectively. The replacement cost of Building A was 6.46 million CNY. Thus, the indices of the restoration cost, $\kappa$, under DBE and MCE were 4.6% and 14.3%, respectively. The level of restoration cost was assessed to be level 1, as shown in Table 1.

(2) The restoration costs of SCs and DSNSCs are relatively lower than those of ASNSCs. As depicted in Fig. 7, the sum of the restoration costs of SCs and DSNSCs account for 21% and 17% under DBE and MCE, respectively. For example, under MCE, the restoration cost of RC columns has the highest proportion among the SCs and DSNSCs, as shown in Fig. 7(b); however, this accounts for only 6.3% of the total restoration cost. This is because that the columns are more prone to damages of DS2 with an MIDR of 0.82%, as shown in Fig. 3(a). The corresponding restoration cost of columns with DS2 is only 207 CNY, as shown in Table 7.

(3) The total restoration cost is mostly caused by the repair of ASNSCs, with proportions of 79% and

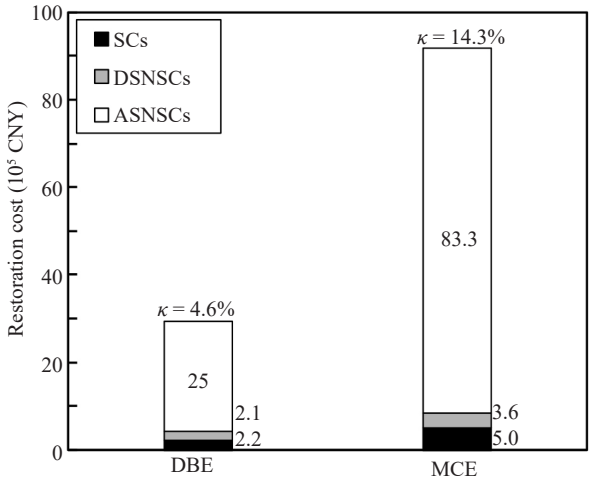


**Fig. 6 Restoration cost of Building A under DBE and MCE**

83% under DBE and MCE, respectively. This is mainly because of the high probability of ASNSCs to attain DS3 as well as the high replacement cost of these components compared with those of SCs and DSNSCs. For example, under MCE, the restoration cost of traction elevators accounts for the largest proportion (41%) of the total cost, as shown in Fig. 7(b). This is because the average MAFA reaches 0.61 g and the possibility for a traction elevator to achieve DS3 is approximately 80% as shown in Fig. 3(c). Moreover, the restoration cost of a traction elevator could be up to 200,000 CNY, as shown in Table 7. Hence, the expectation of a high restoration cost for ASNSCs is dominant.

(4) To improve the level of restoration cost of this building, it is critical to control the MAFA to reduce the damage of ASNSCs.

3.2.3.2 Repair time

According to the standard, repair time estimates include the consideration of both serial and parallel repair strategies. The parallel repair strategy is adopted to repair different floors. In one floor, the serial and parallel repair strategies are both used. Specifically, the SCs and stairs were repaired in parallel as Phase I. Subsequently, other NSCs were serially repaired as Phase II after the completion of Phase I. According to these repair strategies, the longest repair time in a floor, which is the maximum value of the sum of the time consumed by serial work on each floor, is given as total repair time $T_{tot}$. The repair time of Building A under DBE and MCE is illustrated in Fig. 8, and the following conclusions can be drawn from these findings.

(1) The total repair time required for Building A under DBE and MCE is 37.9 and 52.6 days, respectively, both of which are longer than 30 days, leading to a level of 0 as shown in Table 2.

(2) The repair time for Phase I is longer than that for Phase II under DBE and MCE. The repair time of SCs and traction elevators dominates that of Phases I and II, respectively. Notably, the repair time of SCs is longer than that of NSCs. This mainly could be because the quantity of SCs is larger than that of traction elevators. For example, under MCE, the second floor experienced the severest structural damages, leading to a repair time of 6.2 and 5.6 man-days for columns and beams with DS2, respectively; the numbers of columns and beams on this floor were 75 and 67, respectively. According to the standard, two workers per 100 $m^2$ were required to repair the SCs specified, and the area of the floor is approximately 1200 $m^2$. Therefore, the expectation of the corresponding repair time of SCs in the second floor is approximately 39.5 days under MCE. Moreover, only one traction elevator was installed in the building, the repair time of which is 13.1 days for DS3.

(3) The damage of SCs and NSCs both significantly affect the repair time of the building. To improve the level of repair time of this building, it is critical to control the MIDR and MAFA to reduce the damage of SCs and NSCs.

3.2.3.3 Casualties

The indices of casualties, i.e., $\gamma_H$ and $\gamma_D$ of Building A under DBE and MCE are listed in Table 7. According to Table 3, the casualties of Building A are assessed to be at level 1.

Based on the above analyses, the seismic resilience level of Building A was assessed to be level 0 based on the lowest level of the restoration cost, repair time and casualties. Therefore, it is determined to be necessary to improve the seismic resilience of Building A and ensure its function after an earthquake.

**Table 7 Casualties of Building A under DBE and MCE**

| Earthquake level | Hurt ratio, $\gamma_H$ | Death ratio, $\gamma_D$ |
|---|---|---|
| DBE | $2.76\times10^{-5}$ | 0 |
| MCE | $3.61\times10^{-3}$ | $6.29\times10^{-4}$ |

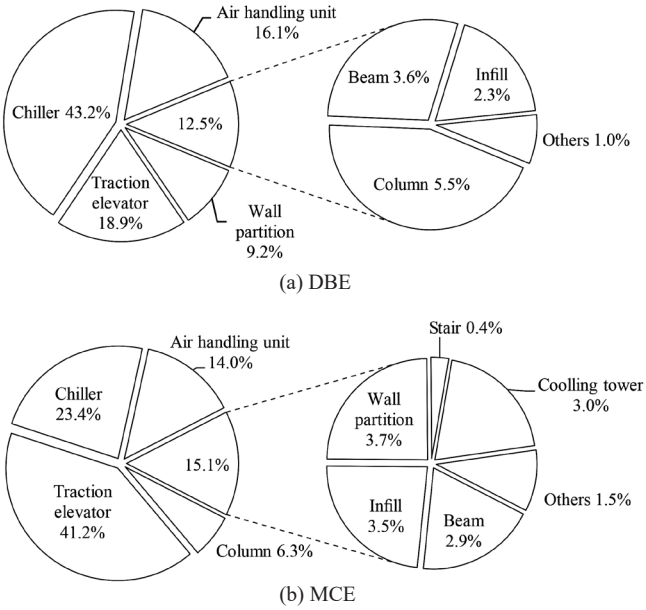


**Fig. 7 Composition of restoration costs for Building A**

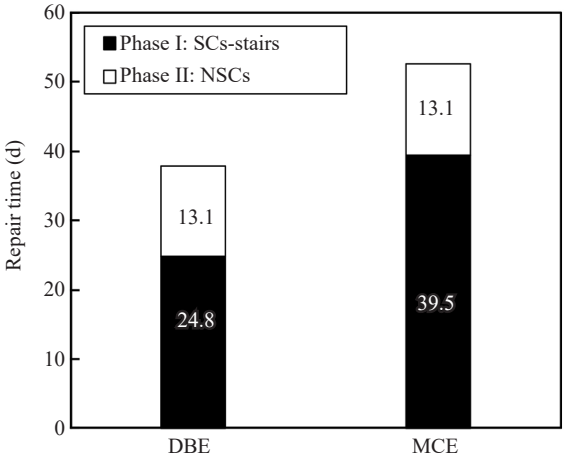


**Fig. 8 Repair time of Building A under DBE and MCE**

### 3.3 Building B

The seismic resilience of Building B was also assessed using the assessment method of the standard. The procedure of the assessment was identical to that for Building A. The critical EDPs of Building B under DBE and MCE are illustrated in Fig. 9. The restoration costs, repair time and casualties of Building B are presented in Fig. 10, Fig. 11, and Table 8, and were assessed to be level 1, level 0, and level 1, respectively. Thus, the seismic resilience level of Building B was also assessed to be level 0. The composition of the restoration costs and repair time of Building B tended to be similar to those of Building A.

Notably, the repair time of Phase I under MCE is 57.4 days, which is longer than that of Building A, i.e., 39.5 days. As mentioned above, the repair time of Phase I is controlled by the repair time of the SCs. The comparison of Figs. 9(a) and 5(a) shows that the MIDR of Building B (1.51%) is larger than that of Building A (0.82%). Thus, the SCs in Building B are more likely to attain DS3 compared to the SCs in Building A. The repair time of SCs with DS3 is much longer than that of SCs with DS2. For example, as illustrated in Fig. 3(a), the probability for columns in Building B attaining DS3 is 44%. Moreover, the repair time of columns with DS2 and DS3 is 6.2 and 9.4 days, respectively. Therefore, the expectation of the repair time of Phase I of Building B is longer than that of Building A.

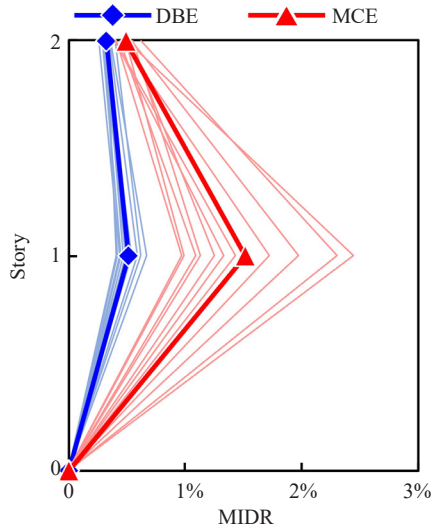


(a) Distribution of MIDR

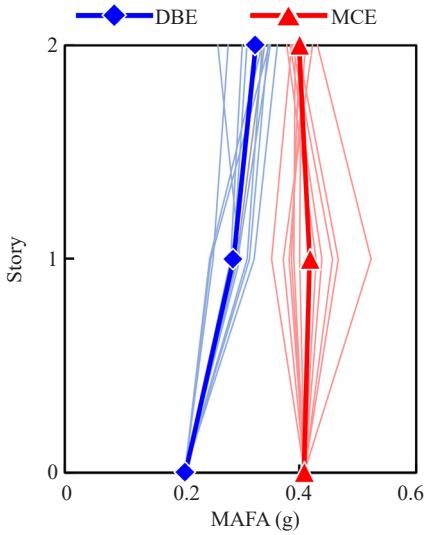


(b) Distribution of MAFA

**Fig. 9 Critical EDPs of Building B under DBE and MCE**

## 4 Seismic resilience of retrofitted RC frame buildings

To improve the seismic resilience of Building A and Building B, seismic isolation is introduced to retrofit these buildings. The corresponding retrofitting schemes

**Table 8 Casualties of Building B under DBE and MCE**

| Earthquake level | Hurt ratio, $\gamma_H$ | Death ratio, $\gamma_D$ |
|---|---|---|
| DBE | $2.76\times10^{-5}$ | 0 |
| MCE | $3.61\times10^{-3}$ | $6.29\times10^{-4}$ |

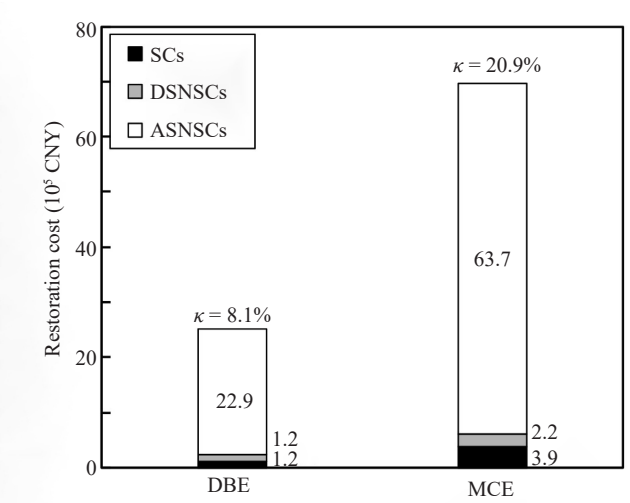


**Fig. 10 Restoration cost of Building B under DBE and MCE**

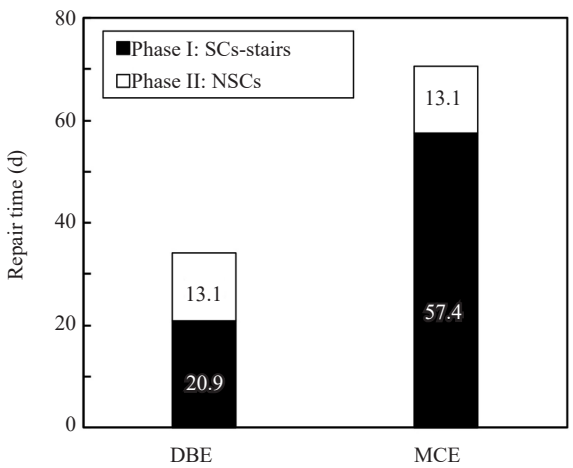


**Fig. 11 Repair time of Building B under DBE and MCE**

are designed according to GB 50011-2010. In addition, the retrofitting scheme, seismic performance, and resilience performance of Building A after retrofitting are discussed in detail, while the critical results of Building B are briefly introduced.

The most important design parameter in seismic isolation is the yield ratio of the isolation system, which significantly affects the efficiency of the isolation system and the seismic performance of the entire building. If seismic resilience is not considered, a yield ratio of 4% is usually used for RC frame structures, and the retrofitting schemes for Building A and Building B are designed according to this value. The retrofitted buildings are named as Building A4 and Building B4. For Building A4, the yield ratio of its isolation system is 4.18%, and the corresponding layout of the bearings is presented in Fig. 12. The dimensions and mechanical properties of lead rubber bearings (LRB) and natural rubber bearings (NRB) adopted in the isolation system are listed in Table 9.

According to GB 50011-2010, the horizontal seismic absorbing coefficient, $\beta$, which indicates the efficiency of the isolation system, is one of the most important indices in the design of seismically isolated structures. This coefficient is defined as the ratio of the maximum shear force of the isolated structure to that of a fixed-base structure on each story under DBE. In addition, the control of the following four critical design indices is required: the maximum bearing displacement (MBD) under MCE, maximum compressive stresses under gravity load ($\sigma_{max}^{g}$), and MCE ($\sigma_{max}^{p}$) as well as maximum tensile stress under MCE ($\sigma_{max}^{t}$). The general-purpose commercial software, ETABS, was used to establish the refined FE model and conduct the seismically isolated designing and NTHAs of the retrofitted buildings. Eleven selected ground motion records in section 4.1.2 were used because the averaged response spectrum also agrees well with the design response spectrum at the fundamental period ($T_{is}$) of Building A4.

**Table 9 Characteristic parameters of the isolators**

| Type | LRB500 | NRB500 | NRB400 |
|---|---|---|---|
| Notation | R5 | N5 | N4 |
| Effective diameter (mm) | 500 | 500 | 400 |
| Total rubber thickness (mm) | 98 | 98 | 78 |
| Equivalent stiffness at 100% shear strain (kN/m) | 1150 | 620 | 490 |
| Post-yield stiffness (kN/m) | 600 | - | - |
| Horizontal yield force (kN) | 73 | - | - |
| Equivalent damping ratio | 0.31 | - | - |
| Diameter of lead core (mm) | 100 | - | - |
| Vertical stiffness (kN/mm) | 2736 | 2017 | 1613 |
| First shape factor | 37 | 35 | 35 |
| Second shape factor | 5.10 | 5.08 | 5.08 |

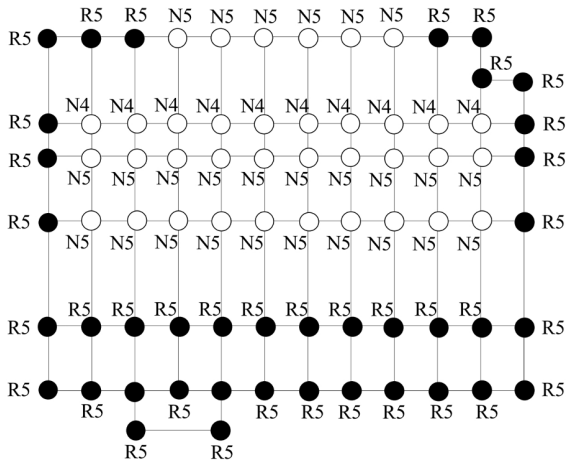


**Fig. 12 Isolation system of Building A4**

The calculated and code-required upper thresholds of these indices of Building A4 are presented in Table 10, indicating that the isolation system of this building meets the design requirements. The critical EDPs of Building A before and after retrofitting under DBE and MCE are compared in Fig. 13. As shown, the MIDR and MAFA are effectively controlled after retrofitting. Furthermore, under MCE, the values of MIDR and MAFA decreased from 0.82% to 0.16% and 0.61 g to 0.24 g, respectively, with the corresponding reduction ratios of 80.5% and 60.9%.

The seismic resilience of Building A4 was also assessed using the above-mentioned method. The restoration cost of Building A4 and its composition are presented in Table 11 and Fig. 14, respectively. By comparing the results obtained before and after the retrofitting, the following findings can be drawn.

(1) The level of restoration cost of Building A was effectively improved from level 1 to level 2 after retrofitting. The indices of the restoration costs ($\kappa$) under DBE and MCE were decreased from 4.6% to 2.3% and 14.3% to 7.2%, respectively, resulting in a level 2 according to Table 1. The restoration cost of Building A4 was mostly caused by the repair of ASNSCs.

(2) The proportion of the restoration cost of ASNSCs was more than 99% under DBE and MCE for Building A4 and is larger than that for Building A. This is because after retrofitting, the MIDR is more effectively controlled

**Table 10 Critical design parameters and indices of Building A4**

| Index | Value | Code requirement |
|---|---|---|
| $T_{is}$ (s) | 2.064 | - |
| $Q_y/W$ (%) | 4.18 | - |
| $\beta$ | 0.3 | ≤ 0.4 |
| MBD (mm) | 146.2 | ≤ 275 |
| $\sigma_{max}^{g}$ (MPa) | 8.4 | ≤ 15 |
| $\sigma_{max}^{p}$ (MPa) | 12.14 | ≤ 30 |
| $\sigma_{max}^{t}$ (MPa) | 0 | ≤ 1 |

than the MAFA. For example, under MCE, the MIDR was effectively reduced from 0.82% to 0.16%. With such an MIDR, the probabilities that the columns and infills attain DS1 are both lower than 10%, as shown in Figs. 3(a) and 3(b). Hence, the expectation of the repair costs of SCs and DSNSCs are effectively reduced. Furthermore, the averaged (maximum) MAFA was reduced from 0.61g (0.71 g) to 0.24g (0.26 g) under MCE. As such, the probabilities that the chillers and traction elevators attain DS3 remain 80% and 15%, respectively, as shown in Fig. 3(c). Therefore, a considerable restoration cost is observed for these ASNSNs, and it dominates the total restoration cost.

The repair time of Building A4 under DBE and MCE is illustrated in Fig. 15. The comparisons between the results of Building A (section 4.1.3.2) and Building A4 reveal the following findings.

(1) After retrofitting, the level of repair time of Building A was improved from level 0 to level 2. The total repair time was decreased from 37.9 to 3.3 days and 52.6 to 15.1 days under DBE and MCE, respectively.

(2) The restoration work of NSCs dominates the repair time of Building A4. This is contrary to the findings on the repair time of Building A, but it is consistent with the findings on the restoration cost of Building A4. This could also be attributed to the fact that the MIDR is effectively reduced, and only negligible damage is observed for the SCs after retrofitting. Nevertheless, the repair time required for chillers and traction elevators is still considerably long after retrofitting, thus hindering the further improvement of the seismic resilience of this building.

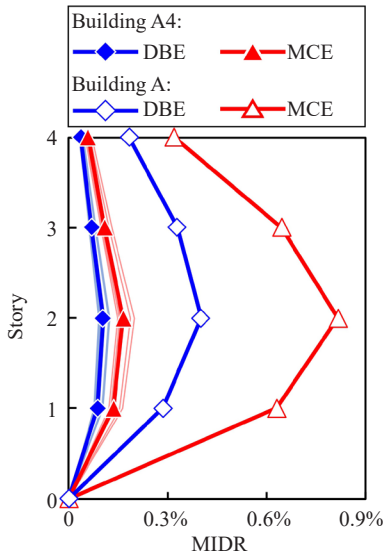


(a) Comparison of the distribution of MIDR

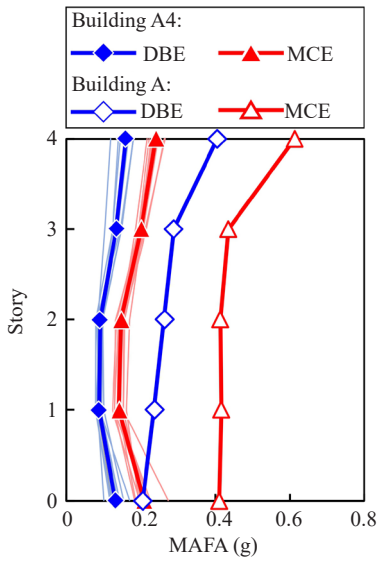


(b) Comparison of the distribution of MAFA

**Fig. 13 Comparisons of the critical EDPs of Building A before and after retrofitting**

**Table 11 Restoration cost of Building A4 under DBE and MCE ($10^5$ CNY)**

| Component type | DBE | MCE |
|---|---|---|
| SC | 0.005 | 0.040 |
| DSNSC | 0.127 | 0.185 |
| ASNSC | 14.584 | 46.136 |
| Total | 14.716 | 46.361 |

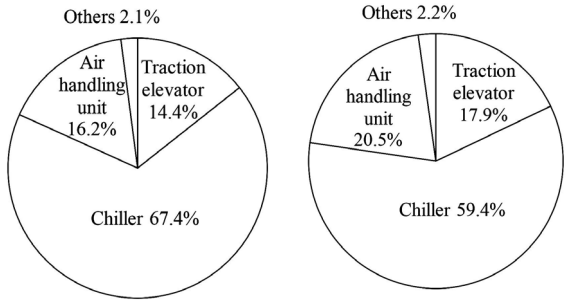


(a) DBE (b) MCE

**Fig. 14 Composition of restoration costs for Building A4 under DBE and MCE**

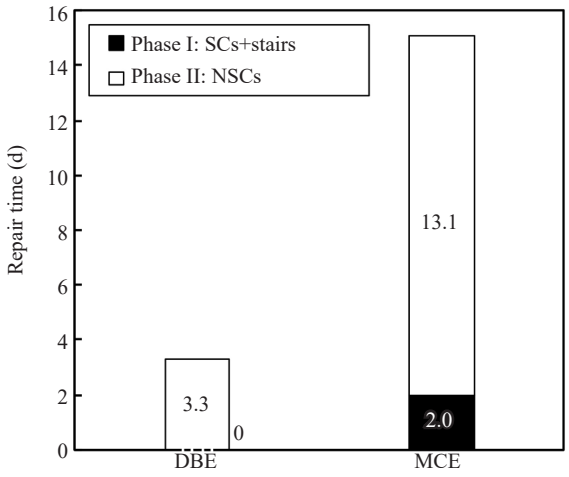


**Fig. 15 Repair time of Building A4 under DBE and MCE**

The hurt ratio ($\gamma_H$) and death ratio ($\gamma_D$) of Building A4 are both 0 under DBE and MCE. The level of casualties is therefore improved from level 1 to 3 after retrofitting.

The above analysis indicates that the seismic resilience of Building A could be improved to level 2 from level 0 after retrofitting. Notably, the restoration cost and repair time of Building A4 are both level 2 because the damage of some ASNSCs is still considerable. To improve the level to level 3, the MAFA of the building must be further controlled. This requires the use of an isolation system with a lower yield ratio.

For Building B4, the yield ratio of its isolation system was also approximately 4%. The isolation system of Building B4 is shown in Fig. 16. The MIDR and MAFA of Buildings B4 and B under MCE are compared in Fig. 17. The levels of restoration costs, repair times, and casualties of Building B4 are 2, 2, and 3, respectively, indicating that the level of seismic resilience of Building B is improved from level 0 to level 2 after retrofitting. The levels of restoration cost and repair time of Building B4 are both level 2 because the damage of some ASNSCs is still considerable.

Based on the above analysis, it can be concluded that retrofitting using seismic isolation is an effective method to improve the seismic resilience of existing RC-frame buildings, because it can significantly reduce the critical EDPs and alleviate the damage states of all components. However, the influence of yield ratio on the isolation efficiency and improvement of seismic resilience must be further investigated.

## 5 Rational yield ratio for resilience-based improvement of existing buildings

### 5.1 Recommendation of rational yield ratio

As mentioned above, it is valuable to recommend a rational yield ratio for the resilience-based improvement of existing buildings using seismic isolation. To achieve this, seismic isolation retrofitting schemes of Building A and Building B with different yield ratios were designed, and the seismic resilience of the retrofitted buildings were evaluated. The considered yield ratios were approximately 3%, 4%, and 5%, resulting in six cases. The critical indices of these six cases are presented and compared in Table 12.

The seismic resilience for these six cases (Table 12) was also assessed according to the standard. The level of casualties of all cases is level 3. The indices of restoration cost and repair time under MCE are illustrated in Fig. 18.

(1) The indices of restoration cost and repair time generally increase with the yield ratio. This trend is consistent with expectations, because the MIDR and MAFA decrease with the increase of yield ratio, as shown in Table 12.

(2) For Building A3 and Building B3, the corresponding indices of restoration cost are both lower than 5%, and their corresponding indices of repair time are less than 7 days. These results indicate that the seismic resilience of buildings retrofitted with a yield ratio of approximately 3% can be successfully improved

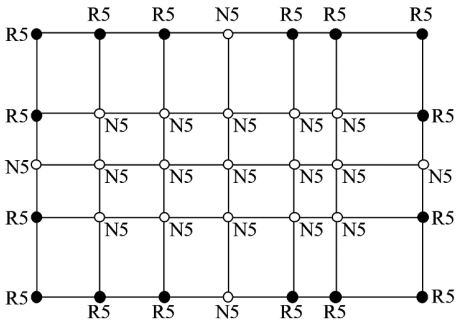


**Fig. 16 Isolation system of Building B4**

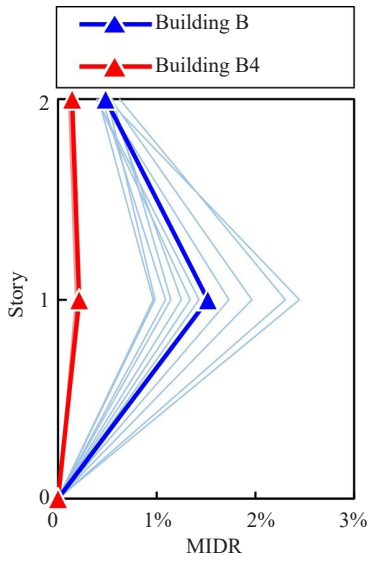


(a) Comparison on the distribution of MIDR

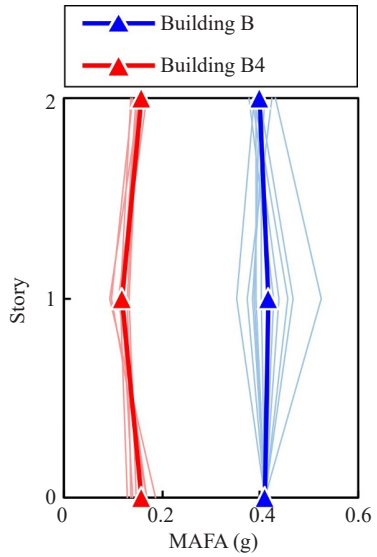


(b) Comparison on the distribution of MAFA

**Fig. 17 Comparisons of the critical EDPs of Building B before and after retrofitting**

to level 3. Notably, the seismic intensities of most cities in China are lower than those in Beijing, and most RC frame buildings in high seismic intensity regions have 2–4 stories. Hence, the yield ratio of 3% can be considered as a rational value if the seismic resilience of level 3 is expected to be achieved.

(3) The seismic resilience of the buildings retrofitted with a yield ratio of approximately 5% also reaches level 2. Note that currently, such a value is approximately the maximum value used in real engineering practices. Hence, the level of seismic resilience of retrofitted RC frame buildings using seismic isolation can basically reach level 2.

### 5.2 Application and validation of the rational yield ratio

To validate the feasibility and reliability of the recommended rational yield ratio (i.e., 3%), another existing RC frame building with four stories was selected and retrofitted. This is an office building located in the urban area of Beijing and is denoted as Building C. The corresponding information of the building is listed in Table 13, and its three-dimensional and planar views are illustrated in Fig. 19. The design seismic intensity of this building is also 8 degrees, and the site condition belongs to Site Class II and the second group. The first three periods of Building C are 0.731 s (1st-order translation in the *Y* direction), 0.691 s (1st-order translation in the *X* direction), and 0.641 s (1st-order torsion), respectively.

The seismic isolation retrofitting scheme of Building C was designed with the recommended yield ratio. The seismic weight of Building C is 80,584 kN. To achieve a yield ratio close to 3%, the required total yield force of the isolation system is approximately 2418 kN. Therefore, 34 R5 with a yield force of 73 kN and 24 N5, as shown in Table 9, were adopted in the isolation system. The total yield force of the isolation system was 2482 kN, and the actual yield ratio was 3.08%. In addition, LRBs were set along the outline of the structure to alleviate the torsion effect. The corresponding layout of the bearings is efficiently determined and illustrated in Fig. 20. The first three periods of Building C after retrofitting were 2.499 s (1st-order translation in the *Y* direction), 2.465 s (1st-order translation in the *X* direction), and 2.136 s (1st-order torsion), respectively. Figure 21 compares the MIDR and MAFA for Building C under MCE before and after retrofitting. The values of MIDR and MAFA are

**Table 12 Critical indices of study cases**

| Notation | Yield ratio (%) | MIDR (%) | MAFA (g) |
|---|---|---|---|
| Building A3 | 3.11 | 0.159 | 0.182 |
| Building A4 | 4.18 | 0.164 | 0.239 |
| Building A5 | 5.14 | 0.168 | 0.269 |
| Building B3 | 3.02 | 0.207 | 0.146 |
| Building B4 | 3.95 | 0.213 | 0.157 |
| Building B5 | 5.12 | 0.224 | 0.171 |

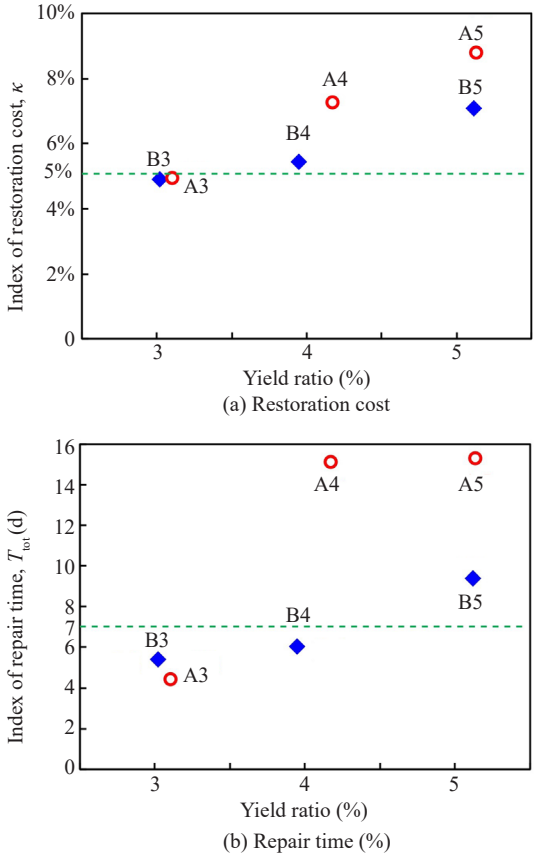


**Fig. 18 Indices of restoration cost and repair time of six cases under MCE**

**Table 13 Main information of Building C**

| Index | Building C |
|---|---|
| Number of floors | 4 |
| Building height (m) | 15.96 |
| Height-to-width ratio | 1.07 |
| Building area ($m^2$) | 4426.8 |
| Replacement cost (CNY) | 6,685,558 |

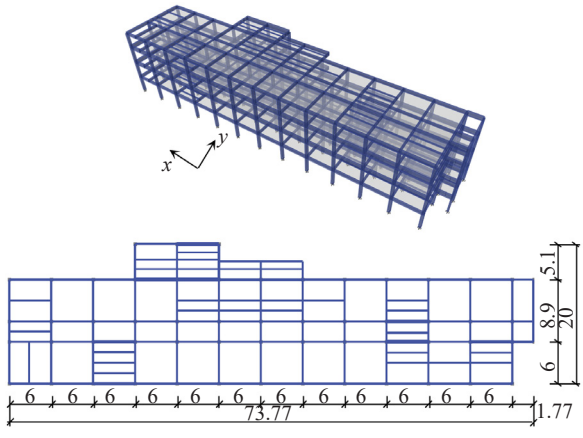


**Fig. 19 Three-dimensional and planar views of Building C (unit: m)**

effectively reduced from 0.82% to 0.2% and 0.46 g to 0.16 g, respectively.

The restoration cost and repair time of Building C before and after retrofitting are illustrated in Figs. 22 and 23, respectively. The level of restoration cost and the level of repair time were both improved from level 1 to level 3. In addition, the level of casualties was also improved from level 1 to level 3. The level of seismic resilience was effectively improved from level 1 to level 3 by introducing an isolation system with a yield ratio of 3.08%. Note that no iteration was conducted during this design process, thus validating the reliability and high efficiency of the recommended value.

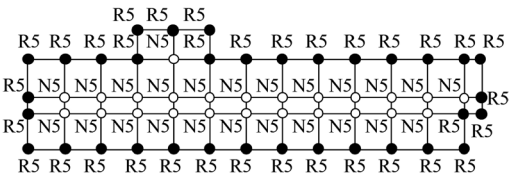


**Fig. 20 Isolation system of Building C after retrofitting**

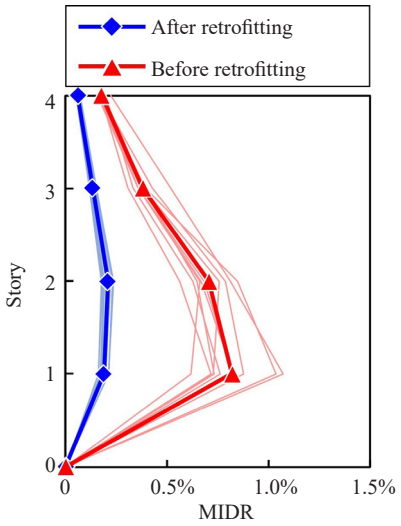


(a) Comparison of the distribution of MIDR

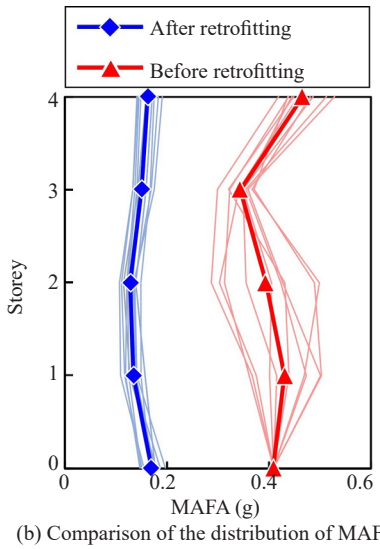


(b) Comparison of the distribution of MAFA

**Fig. 21 Comparisons of the critical EDPs of Building C before and after retrofitting under MCE**

## 6 Conclusion

To quantify and improve the seismic resilience of typical existing RC frame buildings, the seismic resilience of two existing RC frame buildings located in Beijing were assessed based on the Chinese Standard for Seismic Resilience Assessment of Buildings. The critical EDPs affecting the seismic resilience of such buildings were identified. Subsequently, the seismic resilience of retrofitted buildings with different isolation schemes (i.e., yield ratios) was evaluated and compared, with emphasis on the relationships between yield ratios, EDPs, and levels of seismic resilience. Accordingly, to achieve the highest level of seismic resilience with

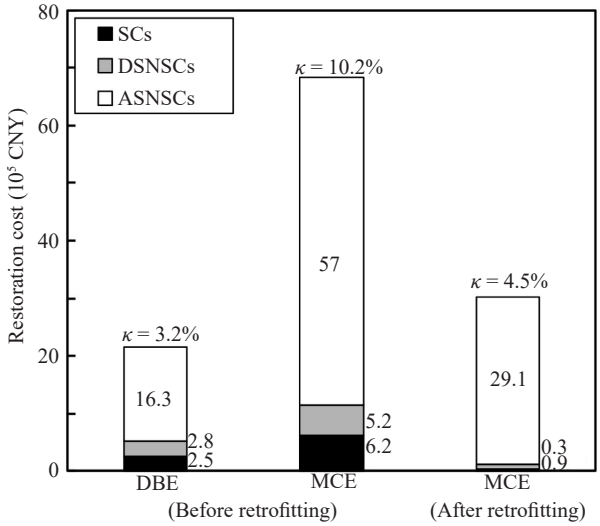


**Fig. 22 Restoration cost of Building C before and after retrofitting**

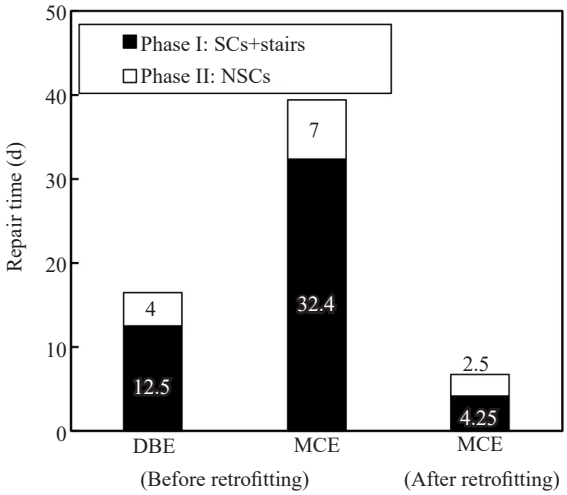


**Fig. 23 Repair time of Building C before and after retrofitting**

respect to the Chinese standard, a rational yield ratio was recommended and successfully applied directly to the design of the seismic resilience improvement of existing RC frame buildings. The following conclusions can be drawn from this study.

(1) The levels of the restoration cost, repair time, and casualties of two selected buildings were 1, 0, and 1, respectively. The corresponding levels of seismic resilience were assessed to be the lowest level of these three aspects, i.e., level 0. MAFA (maximum absolute floor acceleration) was identified as the EDPs affecting the restoration cost. MAFA and MIDR (maximum inter-story drift ratio) were identified as the EDPs affecting the restoration cost and repair time.

(2) Seismic isolation is an effective method to improve the seismic resilience of existing RC frame buildings. After retrofitting, the corresponding levels of seismic resilience were successfully improved to 2 or 3. The MIDR could be significantly reduced after retrofitting, resulting in approximately the complete elimination of the restoration cost and repair time of structural components as well as displacement sensitive non-structural components. In contrast, although a considerable reduction effect was observed for MAFA, the damage of some acceleration sensitive non-structural components could not be completely avoided if the yield ratio was larger than 3%.

(3) The yield ratio of the isolation system is found to be a critical design parameter affecting the seismic resilience of the retrofitted buildings. The levels of restoration cost and repair time increased with the decrease in the yield ratio. For low-rise frame buildings, the rational value of the yield ratio was recommended to be approximately 3% for achieving the highest level (i.e., level 3) of seismic resilience specified by the standard. Under the guidance of this value, the seismic resilience of an RC frame building was successfully and efficiently improved to level 3 without any iterative design, thus validating the feasibility and high efficiency of using this value.

Although a robust value of the yield ratio is required to be investigated, the outcome of the current research could also provide an important reference for the resilience-based retrofitting of existing RC frame buildings using seismic isolation in urban cities.

## Acknowledgement

The authors are grateful for the financial support received from the Beijing Natural Science Foundation (Grant 8192008), the Scientific Research Foundation of Graduate School of Southeast University (YBPY2021), the Science and Technology Project of Beijing Municipal Education Commission (KM201910016014), and the Program for Changjiang Scholars and Innovative Research Team in University (IRT_17R06).

## References

Almufti I and Willford M (2013), *REDi™ Rating System: Resilience-Based Earthquake Design Initiative for the Next Generation of Buildings*, Arup Co, http://publications.arup.com/Publications/R/REDi_Rating_System.aspx.

Avşar Ö and Özdemir G (2013), "Response of Seismic-Isolated Bridges in Relation to Intensity Measures of Ordinary and Pulselike Ground Motions," *Journal of Bridge Engineering*, **18**(3): 250–260.

Bhagat S and Wijeyewickrema AC (2017), "Seismic Response Evaluation of Base-Isolated Reinforced Concrete Buildings Under Bidirectional Excitation," *Earthquake Engineering and Engineering Vibration*, **16**(2): 365–382.

Bruneau M, Chang SE, Eguchi RT, *et al*. (2003), "A Framework to Quantitatively Assess and Enhance the Seismic Resilience of Communities," *Earthquake Spectra*, **19**(4): 733–752.

Cimellaro GP, Malavisi M and Mahin S (2017), "Using Discrete Event Simulation Models to Evaluate Resilience of an Emergency Department," *Journal of Earthquake Engineering*, **21**(2): 203–226.

Cimellaro GP, Reinhorn AM and Bruneau M (2010), "Framework for Analytical Quantification of Disaster Resilience," *Engineering Structures*, **32**(11): 3639–3649.

Computers and Structures Inc. (2003), *ETABS*, Berkeley, USA.

Dong You and Frangopol DM (2016), "Performance-Based Seismic Assessment of Conventional and Base-Isolated Steel Buildings Including Environmental Impact and Resilience," *Earthquake Engineering & Structural Dynamics*, **45**(5): 739–756.

FEMA (2012), *Seismic Performance Assessment of Buildings (Volume 1-Methodology)*, P-58-1, Federal Emergency Management Agency, USA.

Hu Kai, Zhou Ying, Li Jiang, *et al*. (2017), "A Mechanical Tension-resistant Device for Lead Rubber Bearings," *Engineering Structures*, **152**: 238–250.

Li Aiqun (2020), *Vibration Control for Building Structures*, Springer, Switzerland.

Li Aiqun, Yang Cantian, Xie Linin, *et al*. (2017), "Research on the Rational Yield Ratio of Isolation System and its Application to the Design of Seismically Isolated Reinforced Concrete Frame-Core Tube Tall Buildings," *Applied Sciences*, **7**(11): 1191.

Li Xiangzhen, Li Bing, Fu Huangchang, *et al*. (2012), "The Computational Analysis and Evaluation on the Seismic Response of Base Isolated Benchmark Building," *Applied Mechanics and Materials*, **32**(5): 127–135.

Liu Lide (2019), "Research on the Influence of the Yield

Ratio of Isolated RC Frame-Core Tube Tall Buildings in High Intensity Areas," Beijing University of Civil Engineering and Architecture, Beijing. (in Chinese)

Lu Xinzheng, Xie Linlin, Guan Hong, *et al*. (2015), "A Shear Wall Element for Nonlinear Seismic Analysis of Super-Tall Buildings Using OpenSees," *Finite Elements in Analysis and Design*, **98**: 14–25.

Mander JB, Priestley MJN and Park R (1988), "Theoretical Stress-Strain Model for Confined Concrete," *Journal of Structural Engineering*, **114**(8): 1804–1826.

Matsagar VA and Jangid RS (2008), "Base Isolation for Seismic Retrofitting of Structures," *Practice Periodical on Structural Design and Construction*, **13**(4): 175–185.

Mayes RL, Brown AG and Pietra D (2012), "Using Seismic Isolation and Energy Dissipation to Create Earthquake-Resilient Buildings," *Bulletin of the New Zealand Society for Earthquake Engineering*, **45**(3): 117–122.

MOHURD (2020), *Standard for Seismic Resilience Assessment of Buildings*, GB/T 18591-2020, Ministry of Housing and Urban-rural Development, China.

MOHURD (2016), *Code for Seismic Design of Buildings*, GB 50011-2010, Ministry of Housing and Urban-Rural Development, China.

Mollaioli F, Lucchini A, Cheng Yin *et al*. (2013), "Intensity Measures for the Seismic Response Prediction of Base-Isolated Buildings" *Bulletin of Earthquake Engineering*, **11**(5): 1841–1866.

Moretti S, Trozzo A, Terzic V, *et al*. (2014), "Utilizing Base-Isolation Systems to Increase Earthquake Resiliency of Healthcare and School Buildings," *Procedia Economics and Finance*, **18**: 969–976.

Park JG and Otsuka H (1999), "Optimal Yield Level of Bilinear Seismic Isolation Devices," *Earthquake Engineering & Structural Dynamics*, **28**(9): 941–955.

Pourzeynali S and Zarif M (2008), "Multi-Objective Optimization of Seismically Isolated High-Rise Building Structures Using Genetic Algorithms," *Journal of Sound and Vibration*, **311**(3-5): 1141–1160.

Providakis CP (2008), "Effect of LRB Isolators and Supplemental Viscous Dampers on Seismic Isolated Buildings Under Near-Fault Excitations," *Engineering Structures*, **30**(5): 1187–1198.

Renschler CS, Frazier AE, Arendt LA, *et al*. (2010), *A Framework for Defining and Measuring Resilience at the Community Scale: The PEOPLES Resilience Framework*, MCEER Buffalo, NY.

Shang Qingxue, Wang Tao and Li Jichao (2019), "Seismic Fragility of Flexible Pipeline Connections in a Base Isolated Medical Building," *Earthquake Engineering and Engineering Vibration*, **18**(4): 903–916.

Taniguchi M, Fujita K, Tsuji M, *et al*. (2016), "Hybrid Control System for Greater Resilience Using Multiple Isolation and Building Connection," *Frontiers in Built Environment*, **2**: 26.

Tian Yuan, Lu Xiao, Lu Xinzheng, *et al*. (2016), "Quantifying the Seismic Resilience of Two Tall Buildings Designed Using Chinese and US Codes," *Earthquakes and Structures*, **11**(6): 925–942.

Xie Linlin, Lu Xinzheng, Guan Hong, *et al*. (2015), "Experimental Study and Numerical Model Calibration for Earthquake-Induced Collapse of RC Frames with Emphasis on Key Columns, Joints, and the Overall Structure," *Journal of Earthquake Engineering*, **19**(8):1320–1344.

Xiong Chen, Huang Jin and Lu Xinzheng (2020), "Framework for City-Scale Building Seismic Resilience Simulation and Repair Scheduling with Labor Constraints Driven by Time–History Analysis," *Computer-Aided Civil and Infrastructure Engineering*, **35**(4): 322–341.

Yang Cantian, Xie Linlin, Li Aiqun, *et al*. (2019), "Ground Motion Intensity Measures for Seismically Isolated RC Tall Buildings," *Soil Dynamics and Earthquake Engineering*, **125**: 105727.

Yang Cantian, Xie Linlin and Li Aiqun (2019), "Full-Scale Experimental and Numerical Investigations on Seismic Performance of Square RC Frame Columns with Hollow Sections," *Journal of Earthquake Engineering*, doi: 10.1080/13632469.2019.1689869.

Zhou Ying and Chen Peng (2017), "Shaking Table Tests and Numerical Studies on the Effect of Viscous Dampers on an Isolated RC Building by Friction Pendulum Bearings," *Soil Dynamics and Earthquake Engineering*, **100**: 330–344.

Zhou, Ying, Chen Peng, and Gilberto Mosqueda (2019), "Analytical and Numerical Investigation of Quasi-Zero Stiffness Vertical Isolation System," *Journal of Engineering Mechanics*, **145**(6) (2019): 04019035.

Zhou Ying and Chen Peng (2020), "Investigations on a Vertical Isolation System with Quasi-Zero Stiffness Property," *Smart Structures and Systems*, **25**(5): 543–557.

Zhou Fulin and Tan Ping (2018), "Recent Progress and Application on Seismic Isolation Energy Dissipation and Control for Structures in China," *Earthquake Engineering and Engineering Vibration*, **17**(1): 19–27.